

# Accepted Manuscript

Computational and synthetic approaches for developing Lavendustin B derivatives as allosteric inhibitors of HIV-1 integrase

Fatima E. Agharbaoui, Ashley C. Hoyte, Stefania Ferro, Rosaria Gitto, Maria Rosa Buemi, James R. Fuchs, Mamuka Kvaratskhelia, Laura De Luca



PII: S0223-5234(16)30642-0

DOI: [10.1016/j.ejmech.2016.07.077](https://doi.org/10.1016/j.ejmech.2016.07.077)

Reference: EJMECH 8795

To appear in: *European Journal of Medicinal Chemistry*

Received Date: 26 May 2016

Revised Date: 25 July 2016

Accepted Date: 31 July 2016

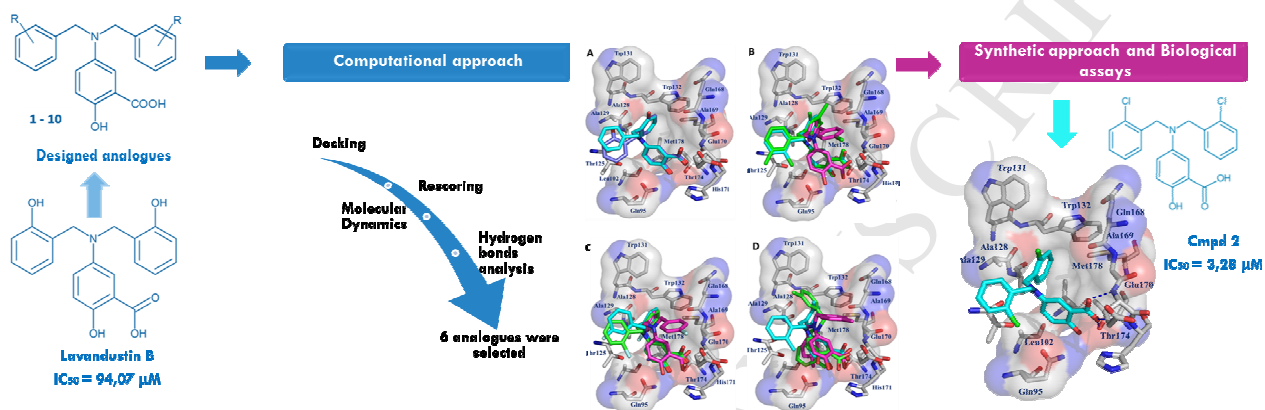
Please cite this article as: F.E. Agharbaoui, A.C. Hoyte, S. Ferro, R. Gitto, M.R. Buemi, J.R. Fuchs, M. Kvaratskhelia, L. De Luca, Computational and synthetic approaches for developing Lavendustin B derivatives as allosteric inhibitors of HIV-1 integrase, *European Journal of Medicinal Chemistry* (2016), doi: 10.1016/j.ejmech.2016.07.077.

This is a PDF file of an unedited manuscript that has been accepted for publication. As a service to our customers we are providing this early version of the manuscript. The manuscript will undergo copyediting, typesetting, and review of the resulting proof before it is published in its final form. Please note that during the production process errors may be discovered which could affect the content, and all legal disclaimers that apply to the journal pertain.

## GRAPHICAL ABSTRACT

## Computational and synthetic approaches for developing Lavendustin B derivatives as allosteric inhibitors of HIV-1 integrase

Fatima E. Agharbaoui<sup>a,b,c</sup>, Ashley C. Hoyte<sup>b</sup>, Stefania Ferro<sup>a</sup>, Rosaria Gitto<sup>a</sup>, Maria Rosa Buemi<sup>a</sup>, James R. Fuchs<sup>c</sup>, Mamuka Kvaratskhelia<sup>b</sup>, Laura De Luca<sup>a,\*</sup>



A computational approach applying docking, rescoring, ultra short MD and hydrogen bonds analysis has been applied for the design and the optimization of Lavendustin B derivatives as IN-LEDGF/p75 inhibitors. The selected derivatives were then synthesized and evaluated using HTRF assays.

## Computational and synthetic approaches for developing Lavendustin B derivatives as allosteric inhibitors of HIV-1 integrase

Fatima E. Agharbaoui<sup>a,b,c</sup>, Ashley C. Hoyte<sup>b</sup>, Stefania Ferro<sup>a</sup>, Rosaria Gitto<sup>a</sup>, Maria Rosa Buemi<sup>a</sup>, James R. Fuchs<sup>c</sup>, Mamuka Kvaratskhelia<sup>b</sup>, Laura De Luca<sup>a,\*</sup>

<sup>a</sup>*Dipartimento di Scienze Chimiche, Biologiche, Farmaceutiche e Ambientali (CHIBIOFARAM) Polo Universitario SS. Annunziata, Università di Messina, Viale Annunziata I-98168 Messina, Italy;* <sup>b</sup>*Center for Retrovirus Research and College of Pharmacy, The Ohio State University, Columbus, OH 43210, USA;* <sup>c</sup>*Division of Medicinal Chemistry and Pharmacognosy, College of Pharmacy, The Ohio State University, Columbus, OH, 43210, USA.*

### Abstract

Through structure-based virtual screening and subsequent activity assays of selected natural products, Lavendustin B was previously identified as an inhibitor of HIV-1 integrase (IN) interaction with its cognate cellular cofactor, lens epithelium-derived growth factor (LEDGF/p75). In order to improve the inhibitory potency we have employed *in silico*-based approaches. Particularly, a series of new analogues was designed and docked into the LEDGF/p75 binding pocket of HIV-1 IN. To identify promising leads we used the Molecular Mechanics energies combined with the Generalized Born and Surface Area continuum solvation (MM-GBSA) method, molecular dynamics simulations and analysis of hydrogen bond occupancies. On the basis of these studies, six analogues of Lavendustin B, containing the benzylamino-hydroxybenzoic scaffold, were selected for synthesis and structure activity-relationship (SAR) studies. Our results demonstrated a good correlation between computational and experimental data, and all six analogues displayed an improved potency for inhibiting IN binding to LEDGF/p75 *in vitro* to respect to the parent compound Lavendustin B. Additionally, these analogs show to inhibit weakly LEDGF/p75-independent IN catalytic activity suggesting a multimodal allosteric mechanism of action. Nevertheless, for the synthesized compounds similar profiles for HIV-1 inhibition and cytotoxicity were highlighted. Taken together, our studies elucidated the mode of action of Lavendustin B analogs and provided a path for their further development as a new promising class of HIV-1 integrase inhibitors.

### Keywords

HIV-1; Integrase; LEDGF/p75; ALLINI; computational studies; IN-LEDGF/p75 binding.

### Abbreviations

allosteric integrase inhibitor (ALLINI); catalytic core domain (CCD); C-terminal domain (CTD) IN-binding domain (IBD); Integrase (IN); Integrase lens epithelium-derived growth factor Allosteric Inhibitors (INLAIs); viral DNA (vDNA); Genetic Optimization for Ligand Docking (GOLD); lens epithelium-derived growth factor (LEDGF/p75); lens epithelium-derived growth factor Integrase Inhibitor (LEDGINs); molecular dynamic (MD); Molecular Mechanics energies combined with the Generalized Born and Surface Area continuum solvation (MM-GBSA), Multimerization Integrase Inhibitors (MINIs); Natural Products (NPs); N-terminal domain (NTD), Non Catalytic Integrase Inhibitors (NCINIs); protein-protein interaction (PPI); protein-protein interaction inhibitors (PPIIs); 3'processing (3'P); strand-transfer (ST); vesicular stomatitis virus g (VSV-g).

\*Corresponding author. E-mail address: [ldeluca@unime.it](mailto:ldeluca@unime.it); [fagharbaoui@unime.it](mailto:fagharbaoui@unime.it)

## 1. Introduction

An essential step of the retroviral lifecycle is the insertion of the reverse-transcribed viral genome into the host chromosome. This process is catalyzed by HIV-1 integrase (IN), that has gained popularity as a promising target for the discovery of novel anti-HIV drugs.

IN is comprised of three domains: the N-terminal domain (NTD), the catalytic core domain (CCD) that coordinates two catalytic  $Mg^{2+}$  ions and the C-terminal domain (CTD) [1, 2]. Initial drug discovery efforts for IN inhibitors have focused on small molecules able to inhibit the catalytic activity of IN and have resulted in three FDA approved IN inhibitors currently in clinical use, raltegravir, elvitegravir and dolutegravir [3-8]. These compounds all share a similar mechanism of action in that all bind at the IN active site in the presence of the viral DNA and inhibit the strand transfer (ST) activity. While these inhibitors have been highly effective against HIV, resistance mutations have emerged in patients [9-11]. Therefore, there is a continual need for the development of new IN inhibitors with innovative scaffolds that target alternative sites of the enzyme.

The integration process comprises two catalytic steps: the first is a hydrolytic reaction termed 3'processing (3' P), followed by a transesterification reaction (also referred as to ST) [12-14]. The cellular chromatin associated protein lens epithelium-derived growth factor (LEDGF/p75) associates with IN and significantly enhances integration efficacy by tethering preintegration complexes to active genes during integration [15-19]. LEDGF/p75 is a transcriptional co-activator strongly associated with chromatin throughout the cell cycle [20-22]. Its C-terminal domain contains the IN-binding domain (IBD), allowing it to not only interact with natural cellular binding partners, but also HIV-1 IN [18, 19, 23, 24].

Recent efforts have led to the discovery of a new class of allosteric IN inhibitors (ALLINIs, also known as LEDGINs, NCINIs, INLAIs, or MINIs) [25-30] targeting the IN dimer interface at the

principal LEDGF/p75 binding pocket. Interestingly, two alternative approaches have identified a similar class of quinoline-based ALLINIs: a high throughput screen was used to discover compounds inhibiting 3'-processing activity of IN [26] and the rational drug design was exploited to develop small molecules to block the IN-LEDGF/p75 interaction [25]. Of note, the rational design approach was made possible by the crystal structure of a CCD-CCD dimer bound to the IBD [31]. Furthermore, the ability to solve the structures of ALLINIs bound at the CCD-CCD dimer [25-28] has facilitated the rapid expansion of this class of inhibitors.

ALLINIs exhibit a multimodal mechanism of action in that they not only inhibit IN-LEDGF/p75 interaction but they also promote higher order aberrant IN multimerization, resulting in inactive protein [2, 32, 33]. Surprisingly, ALLINIs exhibit higher potency when present during virion morphogenesis compared with the early stage of viral replication [29, 34-37]. In the virions, where due to the lack of competing LEDGF/p75 binding to the IN dimer, ALLINIs potently induce aberrant IN multimerization and result in eccentric, non-infectious virions; whereas during the early stage of HIV-1 replication LEDGF/p75 effectively competes with ALLINI binding to IN and reduces the inhibitor potency [38]. Selection of HIV-1 phenotypes under the genetic pressure of various ALLINIs have identified substitutions at the IN dimer interface at the inhibitor binding sites that confer resistance to these compounds [25, 28, 39, 40]. Collectively, the studies with ALLINIs have shown that the potent inhibitors that target IN sites distinct from the active site can be developed. At the same time, there is a need to further improve these compounds to overcome the resistance seen in cell culture assays.

Natural Products (NPs) have historically been an extraordinary source for new medicines and are continuing to be the origin of lead compounds for drug discovery [41, 42]. Previously, we have reported the application of a structure-based virtual screening strategy for the identification of NPs as potential protein-protein interaction inhibitors (PPIIs) targeting the IN-LEDGF/p75 protein complex [43]. Among them, we focused our interest on the Lavendustin B (Figure 1A), which inhibited IN binding to LEDGF/p75 in Alphascreen assay [43]. This novel scaffold is unique from all reported ALLINIs and could represent an encouraging new hit compound warranting further improvement and investigation. Therefore, to exploit this novel scaffold and improve its potency as an IN inhibitor, we have employed *in silico* approaches to identify promising Lavendustin B derivatives and examine inhibitory activities using *in vitro* and *cell based* assays.

## 2. Results and discussion

### 2.1 Rational design

By using a combination of docking and ultrashort molecular dynamics (MD), we have generated a weighted ensemble of protein-ligand configurations for IN-LEDGF/p75 protein-protein interaction inhibitors. Therefore we estimated their binding affinities by averaging snapshots taken from the MD trajectories, together with the presence of fundamental hydrogen bonds [44]. These *in silico* studies, followed by experimental analysis of selected compounds, have led to the identification of Lavendustin B with an  $IC_{50}$  of 94.07  $\mu$ M for inhibiting IN binding to LEDGF/p75 *in vitro* [43]. *In silico* docking studies (Figure 1 B) have highlighted the following interactions: the carboxylic group of Lavendustin B establishes H-bond interactions with the backbone nitrogen atoms of Glu170 and His171 residues, similar to the interactions seen with LEDGF/p75 hotspot residue of Asp366 [24]. Additionally, there is the formation of a potential hydrogen bond with the hydroxyl group side chain of the Thr174 residue. The remaining portion of Lavendustin B is housed within the dimer interface cleft comprised of IN subunit A residues of Thr174, Gln168, Ala169 and Met178 and IN subunit B residues of Ala128, Ala129, Trp131 and Trp132 allowing the molecule to establish hydrophobic contacts with both subunits. We have used these *in silico* predicated interactions as the basis for our current study.

In order to design new analogs, we utilized a published X-ray crystal structure of the active compound KF115 (PDB-400J) which shares a similar binding mode with Lavendustin B (Figure 1A and C) [28]. KF115 is a pyridine-based inhibitor in the class of ALLINIs that preferentially promoted aberrant IN multimerization over inhibiting the IN-LEDGF/p75 interaction. The superimposition of the crystal structure of KF115 bound to the CCD-CCD dimer with the docked model of Lavendustin B (Figure 1B) reveals a high degree of similarity with the carboxylic groups of the both compounds interacting with Glu170, His171 and Thr174. In addition, the 4-chlorophenyl and the 3,4-dimethylphenyl groups of KF115 occupy the hydrophobic pockets in a similar manner of the two 2-hydroxyphenyl portions of Lavendustin B. Considering these results, structural modifications on Lavendustin B were introduced *in silico*: the 2-hydroxy group was removed, and halogen atoms (chlorine and fluorine) and methyl substituent were added to explore the hydrophobic areas. The planned modifications on Lavendustin B are depicted in Figure 1 D for compounds (1-10).

### Figure 1

#### 2.2 Docking and molecular dynamics (MD)

Before carrying out the synthesis of the designed compounds (**1-10**) we wanted to predict the potential binding mode of the analogs by means of the reported computational procedure [43, 45]. First a docking simulation into the principal LEDGF/p75 binding pocket on IN [24] was performed using GOLD (Genetic Optimization for Ligand Docking) [46]. In order to take into account the flexible side chain of residue Gln95 two different conformations of IN CCD were used (PDB ID: 3LPU [25] and 2B4J [32]). More than two clusters were taken for additional analysis. To eliminate potentially unfavorable contacts, the geometry of the system was minimized using the steepest descent algorithm followed by a conjugate gradient. The solvent effects were considered through the generalized Born implicit solvent model. The output complex was employed to estimate ligand binding free energy using the MM-GBSA method. The obtained results for both CCD conformations (complex 1 and 2) are shown in Table 1.

**Table 1**

Since the calculated binding energy of the complex 1 and 2 were similar we decided to consider only the conformation of the protein retrieved by 2B4J (complex 1) for further or more complete analysis. Figure 2 shows the binding orientations of the designed analogs. We observed that six compounds, namely (**1-3**, **5**, **6** and **8**), share the binding mode with parent Lavendustin B. The other derivatives (**4**, **7**, **9** and **10**) assume a binding pose for which they mimic the carboxylic functionality of Lavendustin B but adopt a different orientation for the aromatic portion. Key binding interactions for compound (**2**), which has been selected for subsequent studies, are highlighted in Supplemental Figure 1.

**Figure 2**

The docked complexes were further analyzed using both Ultrashort Molecular Dynamics simulations and sander module of AMBER 11 [47]. Additionally, the models were used to estimate the binding affinities by averaging snapshots taken from the MD trajectories using the MM-GBSA method (Table 1).

By comparing the binding energies compound (**2**) was predicted as the most potent derivative of the series, followed by derivatives (**1**) and (**5**). By contrast, compounds (**4**, **7**, **9** and **10**), which were predicted to bind differently than KF115 or Lavendustin B, displayed the weakest binding energies. Therefore, these compounds were predicted to be less active. To explore this hypothesis, analysis of

hydrogen bond occupancies and distance calculations from the hot spot amino acids in the hydrophobic pocket were carried out using Ptraj module from AMBER11 [47]

**Table 2**

The obtained results (Table 2) show that **(1)** and **(2)** established an extra hydrogen bond interaction with Gln95 residue. Moreover, the carboxylic acid is closer to the hot spot amino acids and has the stronger hydrogen bond occupancies in comparison with Lavendustin B. In contrast, compounds **(4, 7, 9 and 10)** showed the weaker hydrogen bonding abilities, especially with residue His171. Collectively our *in silico* approach, in combination with our previous studies [48], suggested the following criteria for the synthesis. The analogs need to bind to the CCD-CCD dimer in a similar mode to Lavendustin B and KF115. Furthermore, the derivatives are expected to exhibit improved binding energy and higher hydrogen bond occupancies in the binding pocket than parent Lavendustin B. This criterion allowed us select compounds **(1-3, 5, 6 and 8)** for chemical synthesis and *in vitro* evaluation.

### 2.3 Chemistry

The picked 5-(dibenzylamino)-2-hydroxybenzoic acids **(1-3, 5, 6 and 8)** were synthesized following the multistep procedure depicted in scheme 1.

#### Scheme 1

Commercially available 2-hydroxy-5-nitro-benzoic acid **(11)** was reduced, using zinc dust in acid medium, to form the corresponding 5-amino-2-hydroxy-benzoic acid **(12)** with high yield and successively converted into the 5-amino-2-hydroxybenzoate **(13)** by esterification reaction.

In the next step, methyl 5-(benzylamino)-2-hydroxybenzoates **(14-19)** were obtained by reaction of intermediate **13** with the suitable benzaldehyde, by means of a reductive amination, in the presence of sodium cyanoborohydride.

For the synthesis of 5-(dibenzylamino)-2-hydroxybenzoates **(20-25)** the obtained intermediates **(14-19)** were treated in dimethylformamide with the appropriate benzyl bromide and sodium hydride, under argon atmosphere. Finally, the target compounds **(1-3, 5, 6, and 8)** were prepared by hydrolysis in basic medium.

#### 2.4 *In vitro* screening of synthesized compounds **1-3**, **5**, **6** and **8**

All the synthesized derivatives were tested in homogeneous time-resolved fluorescence (HTRF)-based assays to evaluate their inhibitory effects on the IN-LEDGF/p75 binding, LEDGF/p75 dependent integration, and LEDGF/p75 independent 3'-processing activity (Table 3).

**Table 3**

As result all the target compounds were able to inhibit LEDGF/p75 dependent IN activity displaying  $IC_{50}$  values ranging from 3.78  $\mu$ M to 18.50  $\mu$ M (Table 3 and Figure 3B) with (**2**) being the most potent in the series. Since this assay does not delineate whether the inhibitor affected IN binding to LEDGF/p75 or impaired IN activity in a LEDGF/p75 independent manner we conducted additional assays as follow. We firstly tested our analogs for their ability to inhibit IN-LEDGF/p75 binding (Table 3 and Fig 3C). All the tested compounds were able to disrupt IN binding to LEDGF/p75 with  $IC_{50}$  values ranging from 3.28  $\mu$ M to 27.59  $\mu$ M and among them compound (**2**) showed the best activity. In addition, we also analyzed the analogs for their ability to inhibit IN 3'-processing activity in the absence of LEDGF/p75. The obtained data showed a weak inhibitions for compounds **1,2,5** and **6**. The results, summarized in Table 3, show that our compounds were able to impair IN activity. Specifically, derivative (**2**) again displayed the best  $IC_{50}$  value (25.67  $\mu$ M), Figure 3D. Collectively, these results lead us to think that Lavendustin B and its analog 5-[bis(2-chlorobenzyl)amino]-2-hydroxybenzoic acid (**2**) can share a common mechanism of action with pyridine- or quinoline-based ALLINIs. For example, similarly to reported ALLINIs [26-29, 32, 33] compound (**2**) inhibits both LEDGF/p75 dependent and independent activities of IN indicating a multimodal mechanism of action. At the same time we note the following differences. The quinoline-based ALLINIs inhibit IN-LEDGF/p75 binding and IN activity in LEDGF/p75 independent reactions with comparable  $IC_{50}$  values [2, 27, 32, 33]. Pyridine-based ALLINIs are significantly more potent (up to 58-fold) for inducing aberrant IN multimerization in the absence of LEDGF/p75 compared with inhibition of IN-LEDGF/p75 binding [28]. In contrast, compound (**2**) was ~8-fold more potent for inhibiting IN-LEDGF/p75 interactions compared with affecting IN activity in the LEDGF/p75 independent manner. Future studies are warranted to clarify the observed differences between these structurally distinct classes of inhibitors.

**Figure 3***2.5 Antiviral and cytotoxicity assays*

Antiviral activities and cellular toxicity of the most potent analog (**2**) were examined founding similar profiles for HIV-1 inhibition and cytotoxicity (see Figure 4). Unfortunately, these findings do not allow us to delineate any potential antiviral activity of **2** from its cellular toxicity.

**Figure 4****3. Conclusions**

By means of a *in silico* methodology a new series of Lavendustin B analogs were designed. The selected 5-(dibenzylamino)-2-hydroxybenzoic acids (**1-3**, **5**, **6** and **8**) inhibited IN-LEDGF/p75 binding as well as impaired IN activity through allosteric mechanisms, and their improved inhibitory potency has been confirmed using a combination of HTRF-based assays. Additionally, the most active derivative (**2**) exhibited a multimodal mechanism of action, similar to the reported ALLINIs. Unfortunately, compound (**2**) displayed significant cellular toxicity precluding our efforts to delineate its potential antiviral activity.

**4. Experimental section***4.1 Docking simulation*

3D structure of each ligand was constructed using Discovery Studio 2.5.5 [49] and minimized using CHARMM force field, followed by Smart Minimizer algorithm performing 1000 steps of Steepest Descent with a root mean square (RMS) gradient tolerance of 3, followed by Conjugate Gradient minimization, until the RMS gradient for potential energy was less than 0.05 kcal/mol/Å. For docking simulations the crystal structure of the dimeric Catalytic Core Domain (CCD) of HIV-1 IN complexed with the Integrase Binding Domain (IBD) of LEDGF/p75 was retrieved from RCSB Protein Data Bank (PDB:2B4J) [31]. The LEDGF/p75 structure and the water molecules from the X-ray crystallography were removed and the missing hydrogens were replaced. Validation of the docking protocol was performed by docking the native co-crystallized ligands of the two crystal structures with the PDB codes 3LPT and 3LPU, into LEDGF/p75 binding site. The comparison of docking results with the co-crystallized form showed success rates with the docked ligand strictly

superimposed with the crystallized conformation with RMSD = 1.01 Å indicating that the used scoring function is successful. These values were small enough and supported the hypothesis that experimental binding modes could be reproduced with accuracy using this protocol. The standard default settings were used in all calculations. Docking studies were performed using the genetic optimization for ligand docking (GOLD) software package version 4.1.1 from the Cambridge Crystallographic Data Centre (CCDC) [46] and as described in our previous paper [48]. For the prediction of ligand binding positions GoldScore fitness function was used. For each ligand 100 independent runs and a maximum of 15000 genetic operations were performed using the default operator weights and a population size of 100 chromosomes. Default cutoff values of 2.5 Å for hydrogen bonds and 4.0 Å for van der Waals interactions were employed. Automatic bond settings were used, allowing the torsion angles of all acyclic, rotatable bonds in the ligand to vary except for amide bonds. Results differing by less than 0.75 Å in ligand-all-atom RMSD were clustered together. Results differing by less than 1.00 Å in ligand-all atom RMSD were clustered together. A 20.0 Å radius active site was drawn on the original position of the LEDGF/p75 IBD dipeptide Ile365-Asp366 and automated cavity detection was used. Two hydrogen bond constraints were used to specify that two protein atoms should be hydrogen-bonded to the ligand, namely NH backbone of Glu170 and His171 with a constraint weight of 5. Binding energy of the minimized complex was calculated using the MM-GBSA method [50] implemented in the AMBER program.

#### 4.2 Molecular dynamic simulation

The starting model for simulations of IN-LEDGF/p75 was prepared as described in our previous paper [48]. In brief, from the X-ray structure 2B4J of IN CCD (chains A and B) in complex with the IBD of LEDGF (chains C and D) [31] was used. First, chain D and water molecules were removed from the structure. Then, the missing residues of the CCD of IN were added by superimposing chain C of the HIV-1 IN 1BL3 [51] structure and energy-minimized using Maestro [52] with a RMSD of 0.30 Å. From the resulting complex, the chain C of IBD of LEDGF/p75 was castoff in order to simulate IN-inhibitor complexes. MD simulations were carried out using the sander module of AMBER 11 [53] and parm 99.dat and frcmod.ff03 parameter files [54, 55]. These parameters were assigned to the designed ligands, while partial charges were calculated using the AM1-BCC method as implemented in the Antechamber suite of AMBER 11. The geometry of the system was minimized in order to remove any bad contacts using the steepest descent algorithm for the first 250 steps before switching to the conjugate gradient algorithm for the remaining 250 steps. Solvent effects were taken into account by using the generalized Born implicit solvent model. The

minimized structure was the input for MD runs using constant-temperature Langevin dynamics at 300 K for 100 ps with a time step of 1fs and a distance cutoff of 12.0 Å for the nonbonded interactions. Snapshots of the complexes during the simulations and the average structures were obtained with the Ptraj module of the AMBER 11 suite [53]. The hydrogen bonds were detected when the acceptor-donor atom distance was lower than 3.5 Å and the acceptor-H-donor angle was more than 120°. The MM-GBSA method [50] implemented in the AMBER program was used to evaluate the ligand-protein interaction free energies of the minimized complex and the 100 snapshots extracted at 1 ps intervals. For MM-GBSA analysis, snapshots at 40 ps intervals were extracted from the last 4 ns of the MD trajectory, and the binding free energies were averaged over the ensemble of conformers produced (100 snapshots for each trajectory).

### 4.3 Chemistry

All starting materials and reagents commercially available (Sigma-Aldrich and Alfa Aesar) were used without further purification. Anhydrous solvents CH<sub>3</sub>OH, DMSO, CH<sub>2</sub>Cl<sub>2</sub>, THF and DMF were used directly from their Sure-Seal bottles and were purchased from Sigma Aldrich. 4Å molecular sieves also purchased from Sigma Aldrich, were activated by heating to 300°C under vacuum overnight. All reactions were performed in oven-dried glassware and were monitored for completeness by thin layer chromatography (TLC) using silica gel then visualized by UV light, or developed by treatment with KMnO<sub>4</sub> stain. A 300MHz Bruker NMR was utilized to obtain <sup>1</sup>H and <sup>13</sup>C NMR spectra in CDCl<sub>3</sub> or DMSO-d<sub>6</sub>. All NMR chemical shifts ( $\delta$ ) are reported in parts per million after calibrations to residual isotopic solvent and coupling constants ( $J$ ) are reported in Hz. All exchangeable protons were confirmed by addition of D<sub>2</sub>O. Melting points were determined on a BUCHI Melting Point B-545 apparatus and are uncorrected. Mass spectrometry analysis were realized on Bruker MicrOTOF (ESI) equipped with and Agilent 1200 LC.

#### *Procedure for the synthesis of 5-amino-2-hydroxy-benzoic acid (12)*

A mixture of 2-hydroxy-5-nitrobenzoic acid (1 mmol, 183 mg) and conc. hydrochloric acid (18 ml) was placed in an ice bath water. Zinc powder (3 mmol, 196 mg) was added dropwise through condenser and the reaction was refluxed for 4 h. Then the mixture was cooled to room temperature, diluted with water and washed with ethyl acetate (3 x 25ml). The obtained organic solution was evaporated in vacuum to give the crude product. The residue was purified by crystallization with diethyl ether. Yield: 88%, Mp: 280-282°C. <sup>1</sup>HNMR, (DMSO-d<sub>6</sub>):  $\delta$  = 6.70 (dd,  $J$ =8.8,  $J$ =1.8, 1H,

ArH), 6.92 (dd,  $J=8.8$ ,  $J=2.9$ , 1H, ArH), 7.24 (s, 1H, ArH). Anal. Calcd for  $C_7H_7NO_3$ : C(54.90%) H(4.61%) N(9.15%). Found: C: 54.80; H: 4.50, N: 9.10.

*Procedure for the synthesis of methyl 5-amino-2-hydroxybenzoate (13)*

To a solution of 5-amino-2-hydroxybenzoic acid (20 mmol, 3.062 g) in methanol (40 mL) sulfuric acid (4.5 mL) was added at 0°C. The reaction mixture was refluxed at 80 °C for 24 h. The solvent was then removed, the reaction mixture was neutralized with saturated sodium bicarbonate aqueous solution until pH =7. The product was extracted with ethyl acetate (3 x 25ml), the organic layers were combined, dried over anhydrous  $Na_2SO_4$  and concentrated to provide the methyl 5-amino-2-hydroxybenzoate (**13**) as a pale yellow solid. Yield: 90%, Mp: 97-99 °C.  $^1H$ NMR, (DMSO- $d_6$ ):  $\delta$  = 3.87 (s, 3H,  $CH_3$ ), 6.92 (d,  $J=8.2$ , 1H, ArH), 7.15 (m, 1H, ArH), 7.39 (m, 1H, ArH), 10.18 (bs, 1H, OH). Anal. Calcd for  $C_8H_9NO_3$  : C(57.48%) H(5.43%) N(8.38%). Found: C: 57.67; H: 5.63, N: 8.34.

*General procedure for the synthesis of methyl 5-(benzylamino)-2-hydroxybenzoates (14-19)*

To a stirred solution of methyl 5-amino-2-hydroxybenzoate (**13**) (1.49 mmol, 250 mg) in MeOH (7ml), over 4A° molecular sieves, benzaldehyde (1.49 mmol, 0.151 ml) and AcOH (0.159 ml) were added. The mixture was heated at 40°C and agitated for 30 min. Then it was stirred for 1h at room temperature. The solution was cooled to 5-10°C and  $NaCNBH_3$  (1.94 mmol, 121 mg), was slowly added. The resulted mixture was stirred for 2h at room temperature before being quenched by the addition of water. The solvent was evaporated under pressure and the crude mixture was taken up in  $CH_2Cl_2$ , washed with water and brine, dried ( $Na_2SO_4$ ) and evaporated. The residue was purified by chromatography (eluent: Hexane/Ethyl acetate: 8/2) to give intermediates **14-19**.

*Methyl 5-(benzylamino)-2-hydroxybenzoate (14)* Yield: 67%, Oil.  $^1H$ NMR, ( $CDCl_3$ ):  $\delta$  = 3.87 (s, 3H,  $CH_3$ ), 4.25 (s, 2H,  $CH_2$ ), 6.79-6.87 (m, 2H, ArH), 7.09 (s, 1H, ArH), 7.28-7.36 (m, 5H, ArH), 10.24 (bs, 1H, OH). Anal. Calcd for  $C_{15}H_{15}NO_3$  : C(70.02%) H(5.88%) N(5.44%). Found: C: 70.12; H: 5.80, N: 5.54.

*Methyl 5-[(2-chlorobenzyl)amino]-2-hydroxybenzoate (15)* Yield: 66%, Oil.  $^1H$ NMR, ( $CDCl_3$ ):  $\delta$  = 4.07 (s, 3H,  $CH_3$ ), 4.57 (s, 2H,  $CH_2$ ), 7.03 (s, 2H, ArH), 7.21-7.46 (m, 4H, ArH), 7.55 (m, 1H, ArH), 10.38 (bs, 1H, OH). Anal. Calcd for  $C_{15}H_{14}ClNO_3$  : C(61.76%) H(4.84%) N(4.80%). Found: C: 61.76; H: 4.84, N: 4.80.

*Methyl 5-[(3-chlorobenzyl)amino]-2-hydroxybenzoate (16)* Yield: 62%, Oil. <sup>1</sup>HNMR, (CDCl<sub>3</sub>):  $\delta$  = 3.93 (s, 3H, CH<sub>3</sub>), 4.28 (s, 2H, CH<sub>2</sub>), 6.81-6.89 (m, 2H, ArH), 7.07 (s, 1H, ArH), 7.25-7.29 (m, 3H, ArH), 7.38 (s, 1H, ArH), 10.21 (bs, 1H, OH). Anal. Calcd for C<sub>15</sub>H<sub>14</sub>ClNO<sub>3</sub>: C(61.76%) H(4.84%) N(4.80%). Found: C: 61.59; H: 4.73, N: 4.68.

*Methyl 5-[(2-fluorobenzyl)amino]-2-hydroxybenzoate (17)* Yield: 65%, Oil. <sup>1</sup>HNMR, (CDCl<sub>3</sub>):  $\delta$  = 4.08 (s, 3H, CH<sub>3</sub>), 4.52 (s, 2H, CH<sub>2</sub>), 7.02 (s, 2H, ArH), 7.20-7.29 (m, 3H, ArH) 7.39-7.55 (m, 2H, ArH), 10.36 (bs, 1H, OH). Anal. Calcd for C<sub>15</sub>H<sub>14</sub>FNO<sub>3</sub>: C(65.45%) H(5.13%) N(5.09%). Found: C: 65.37; H: 5.01, N: 4.97.

*Methyl 5-[(3-fluorobenzyl)amino]-2-hydroxybenzoate (18)* Yield: 62%, Oil. <sup>1</sup>HNMR, (CDCl<sub>3</sub>):  $\delta$  = 3.91 (s, 3H, CH<sub>3</sub>), 4.27 (s, 2H, CH<sub>2</sub>), 6.80-6.87 (m, 2H, ArH), 7.06 (s, 1H, ArH), 7.22-7.41 (m, 4H, ArH), 10.19 (s, 1H, OH). Anal. Calcd for C<sub>15</sub>H<sub>14</sub>FNO<sub>3</sub>: C(65.45%) H(5.13%) N(5.09%). Found: C: 65.37; H: 5.01, N: 4.97.

*Methyl 2-hydroxy-5-[(2-methylbenzyl)amino]benzoate (19)* Yield: 63%, Oil. <sup>1</sup>HNMR, (CDCl<sub>3</sub>):  $\delta$  = 2.30 (s, 3H, CH<sub>3</sub>), 3.84 (s, 3H, CH<sub>3</sub>), 4.50 (s, 2H, CH<sub>2</sub>), 6.80-6.86 (m, 2H, ArH), 7.05-7.14 (m, 2H, ArH), 7.30-7.36 (m, 3H, ArH), 10.21 (bs, 1H, OH). Anal. Calcd for C<sub>16</sub>H<sub>17</sub>NO<sub>3</sub>: C(70.83%) H(6.32%) N(5.16%). Found: C: 70.68; H: 6.21, N: 5.29.

#### *General procedure for the synthesis of methyl 5-(dibenzylamino)-2-hydroxybenzoates (20-25)*

The appropriate methyl 5-(benzylamino)-2-hydroxybenzoate (**14-19**) (0.3 mmol) was dissolved in anhydrous DMF and was added under argon to a suspension of NaH (0.3 mmol, 29 mg) in anhydrous DMF. The reaction mixture was stirred at 0°C under for few minutes, followed by the addition of a solution of suitable benzyl bromide (0.4 mmol) in anhydrous DMF. After 3 h, the reaction mixture was extracted by ethyl acetate (3 x 30ml) and washed with water (2 x 20ml) then with brine (2 x 20ml). The organic layer was dried (Na<sub>2</sub>SO<sub>4</sub>), filtered and the solvent removed under reduced pressure. The resultant product was purified via flash chromatography (Hexane/Ethyl acetate: 98/2) affording the title compounds **20-25**.

*Methyl 5-(dibenzylamino)-2-hydroxybenzoate (20)* Yield: 65%, Mp: 159-161 °C. <sup>1</sup>HNMR, (CDCl<sub>3</sub>):  $\delta$ =3.68 (s, 3H, CH<sub>3</sub>), 4.53 (s, 4H, CH<sub>2</sub>), 6.85 (d, *J*=9.0, 1H, ArH), 7.00 (dd, *J*=9.0, *J*=3.2, 1H, ArH), 7.24-7.36 (m, 11H, ArH), 10.18 (bs, 1H, OH). Anal. Calcd for C<sub>22</sub>H<sub>21</sub>NO<sub>3</sub>: C(76.06%) H(6.09%) N(4.03%). Found: C: 75.09; H: 6.06, N: 4.13.

*Methyl 5-[bis(2-chlorobenzyl)amino]-2-hydroxybenzoate (21)* Yield: 62%, Mp: 175-177 °C. <sup>1</sup>HNMR, (CDCl<sub>3</sub>):  $\delta$  = 3.87 (s, 3H, CH<sub>3</sub>), 4.66 (s, 4H, CH<sub>2</sub>), 6.83 (m, 2H, ArH), 7.09 (m, 1H, ArH),

7.20-7.28 (m, 6H, ArH), 7.38-7.43 (m, 2H, ArH), 10.17 (bs, 1H, OH). Anal. Calcd for  $C_{22}H_{19}Cl_2NO_3$ : C(63.47%) H(4.60%) N(3.36%). Found: C: 63.28; H: 4.54, N: 3.52.

*Methyl 5-[bis(3-chlorobenzyl)amino]-2-hydroxybenzoate (22)* Yield: 60%, Mp: 179-181 °C.  $^1H$ NMR, ( $CDCl_3$ ):  $\delta$  = 3.93 (s, 3H,  $CH_3$ ), 4.50 (s, 4H,  $CH_2$ ), 6.89 (d,  $J=9.1$ , 1H, ArH), 7.00 (dd,  $J=9.1$ ,  $J=3.0$ , 1H, ArH), 7.13-7.18 (m, 2H, ArH), 7.24-7.32 (m, 7H, ArH), 10.25 (bs, 1H, OH). Anal. Calcd for  $C_{22}H_{19}Cl_2NO_3$ : C(63.47%) H(4.60%) N(3.36%). Found: C: 63.57; H: 4.50, N: 3.12.

*Methyl 5-[bis(2-fluorobenzyl)amino]-2-hydroxybenzoate (23)* Yield: 61%, Mp: 177-179 °C.  $^1H$ NMR, ( $CDCl_3$ ):  $\delta$  = 3.92 (s, 3H,  $CH_3$ ), 4.63 (s, 4H,  $CH_2$ ), 6.87 (d,  $J=9.2$ , 1H, ArH), 7.00 (dd,  $J=9.2$ ,  $J=3.2$ , 1H, ArH), 7.05-7.13 (m, 5H, ArH), 7.24-7.30 (m, 2H, ArH), 7.28-7.30 (m, 2H, ArH), 10.22 (bs, 1H, OH). Anal. Calcd for  $C_{22}H_{19}F_2NO_3$ : C(68.92%) H(5.00%) N(3.65%). Found: C: 68.74; H: 4.93, N: 3.32.

*Methyl 5-[bis(3-fluorobenzyl)amino]-2-hydroxybenzoate (24)* Yield: 58%, Mp: 172-174 °C.  $^1H$ NMR, ( $CDCl_3$ ):  $\delta$  = 3.92 (s, 3H,  $CH_3$ ), 4.51 (s, 4H,  $CH_2$ ), 6.89 (d,  $J=9.1$ , 1H, ArH), 7.00 (dd,  $J=9.1$ ,  $J=3.0$ , 1H, ArH), 7.14-7.17 (m, 2H, ArH), 7.25-7.32 (m, 7H, ArH), 10.27 (bs, 1H, OH). Anal. Calcd for  $C_{22}H_{19}F_2NO_3$ : C(68.92%) H(5.00%) N(3.65%). Found: C: 68.79; H: 4.98, N: 3.45.

*Methyl 5-[bis(2-methylbenzyl)amino]-2-hydroxybenzoate (25)* Yield: 61%, Mp: 164-166 °C.  $^1H$ NMR, ( $CDCl_3$ ):  $\delta$  = 2.37 (s, 6H,  $CH_3$ ), 3.95 (s, 3H,  $CH_3$ ), 4.60 (s, 4H,  $CH_2$ ), 6.91 (s, 1H, ArH), 6.92 (s, 1H, ArH), 7.19-7.37 (m, 9H, ArH), 10.27 (bs, 1H, OH). Anal. Calcd for  $C_{24}H_{25}NO_3$ : C(76.77%) H(6.71%) N(3.73%). Found: C: 76.65; H: 6.68, N: 3.89.

#### *General procedure for the synthesis of 5-(dibenzylamino)-2-hydroxybenzoic acids (1-3, 5-6 and 8)*

The appropriate methyl-2-hydroxybenzoate (**20-25**) was dissolved in a mixture of THF (2 ml) and MeOH (2 ml), and 2M NaOH (4 ml) was added. The reaction was refluxed for 24h. After this time the solvent was removed under reduced pressure and the residue was acidified to pH 2 with 2N HCl. The solution was extracted with ethyl acetate (3 x 10ml), dried over  $Na_2SO_4$ , filtered and the solvent removed under reduced pressure. The final products (**1-3**, **5-6** and **8**) were crystallized with a mixture of Hexane/Ethyl acetate/Ethanol (1/1/1) and some drops of methanol.

*5-(Dibenzylamino)-2-hydroxybenzoic acid (1)* Yield: 59%, Mp: 140-142 °C.  $^1H$ NMR, ( $DMSO-d_6$ ):  $\delta$  = 4.60 (s, 4H,  $CH_2$ ), 6.76 (d,  $J = 9$ , 1H, ArH), 7.00 (dd,  $J = 9$ ,  $J = 3.2$ , 1H, ArH), 7.05 (s, 1H, ArH), 7.23-7.35 (m, 10H, ArH), 10.53 (bs, 1H, OH), 13.65 (bs, 1H, OH). Anal. Calcd for  $C_{21}H_{19}NO_3$ : C(75.66%) H(5.74%) N(4.20%). Found: C: 75.54; H: 5.60, N: 4.15. ESI(+),  $CH_3OH$ , HR-MS : ion  $[M+H]^+$ ,  $m/z$  333,  $C_{21}H_{19}NO_3$ ,  $m/z$  theory 333,1365,  $m/z$  found 334,14326.

*5-[Bis(2-chlorobenzyl)amino]-2-hydroxybenzoic acid (2)* Yield: 53%, Mp: 148-150 °C. <sup>1</sup>HNMR, (DMSO-d<sub>6</sub>): δ = 4.68 (s, 4H, CH<sub>2</sub>), 6.75-6.84 (m, 2H, ArH), 6.94 (s, 1H, ArH), 7.23-7.31 (m, 6H, ArH), 7.47 (m, 2H, ArH). Anal. Calcd for C<sub>21</sub>H<sub>17</sub>Cl<sub>2</sub>NO<sub>3</sub>: C(62.70%) H(4.26%) N(3.48%). Found: C: 62.58; H: 4.35, N: 3.35. ESI(+), CH<sub>3</sub>OH, HR-MS : ion [M+H]<sup>+</sup>, m/z 401, C<sub>21</sub>H<sub>17</sub>Cl<sub>2</sub>NO<sub>3</sub>, m/z theory 401,0585, m/z found 402,0651.

*5-[Bis(3-chlorobenzyl)amino]-2-hydroxybenzoic acid (3)* Yield: 50%, Mp: 147-149 °C. <sup>1</sup>HNMR, (DMSO-d<sub>6</sub>): δ = 4.64 (s, 4H, CH<sub>2</sub>), 6.78 (d, *J* = 8.9, 1H, ArH), 6.97- 7.05 (m, 2H, ArH), 7.21-7.39 (m, 8H, ArH), 10.55 (bs, 1H, OH). Anal. Calcd for C<sub>21</sub>H<sub>17</sub>Cl<sub>2</sub>NO<sub>3</sub>: C(62.70%) H(4.26%) N(3.48%). Found: C: 62.86; H: 4.10, N: 3.25. ESI(+), CH<sub>3</sub>OH, HR-MS : ion [M+H]<sup>+</sup>, m/z 401, C<sub>21</sub>H<sub>17</sub>Cl<sub>2</sub>NO<sub>3</sub>, m/z theory 401,0585, m/z found 402,0651.

*5-[Bis(2-fluorobenzyl)amino]-2-hydroxybenzoic acid (5)* Yield: 52%, Mp: 137-139 °C, <sup>1</sup>HNMR, (DMSO-d<sub>6</sub>): δ = 4.65 (s, 4H, CH<sub>2</sub>), 6.79 (d, *J* = 9.1, 1H, ArH), 6.99 (dd, *J* = 9.1, *J* = 3.2, 1H, ArH), 7.06-7.34 (m, 9H, ArH), 10.59 (bs, 1H, OH), 13.69 (bs, 1H, OH). Anal. Calcd for C<sub>21</sub>H<sub>17</sub>F<sub>2</sub>NO<sub>3</sub> : C(68.29%) H(4.64%) N(3.79%). Found: C: 68.07; H: 4.46, N: 3.58. ESI(+), CH<sub>3</sub>OH, HR-MS : ion [M+H]<sup>+</sup>, m/z 369, C<sub>21</sub>H<sub>17</sub>F<sub>2</sub>NO<sub>3</sub>, m/z theory 369,3678, m/z found 370,1241.

*5-[Bis(3-fluorobenzyl)amino]-2-hydroxybenzoic acid (6)* Yield: 49%, Mp: 141-143 °C <sup>1</sup>HNMR, (DMSO-d<sub>6</sub>): δ = 4.63 (s, 4H, CH<sub>2</sub>), 6.78 (d, *J* = 8.8, 1H, ArH), 6.99 (dd, *J* = 8.8, *J* = 3.2, 1H, ArH), 7.04 (d, *J* = 3.2, 1H, ArH), 7.20-7.38 (m, 8H, ArH), 10.52 (bs, 1H, OH), 13.69 (bs, 1H, OH). Anal. Calcd for C<sub>21</sub>H<sub>17</sub>F<sub>2</sub>NO<sub>3</sub> : C(68.29%) H(4.64%) N(3.79%). Found: C: 68.14; H: 4.59, N: 3.61. ESI(+), CH<sub>3</sub>OH, HR-MS : ion [M+H]<sup>+</sup>, m/z 369, C<sub>21</sub>H<sub>17</sub>F<sub>2</sub>NO<sub>3</sub>, m/z theory 369,3678, m/z found 370,1249.

*5-[Bis(2-methylbenzyl)amino]-2-hydroxybenzoic acid (8)* Yield: 48%, Mp: 136-138 °C. <sup>1</sup>HNMR, (CDCl<sub>3</sub>): δ = 2.28 (s, 6H, CH<sub>3</sub>), 4.53 (s, 4H, CH<sub>2</sub>), 6.83 (d, *J* = 9.2, 1H, ArH), 7.85 (m, 1H, ArH) 7.14-7.20 (m, 9H, ArH), 9.79 (bs, 1H, OH). Anal. Calcd for C<sub>23</sub>H<sub>23</sub>NO<sub>3</sub>: C(76.43%) H(6.41%) N(3.88%). Found: C: 76.26; H: 6.30, N: 3.95. ESI(+), CH<sub>3</sub>OH, HR-MS : ion [M+H]<sup>+</sup>, m/z 361, C<sub>23</sub>H<sub>23</sub>NO<sub>3</sub>, m/z theory 361,1678, m/z found 362,1745.

#### 4.4 Recombinant proteins and HTRF-based Assays

His-tagged LEDGF/p75, FLAG-tagged IN and His-tagged IN were constructed and purified as described previously [32]. Homogeneous time resolved fluorescence energy transfer (HTRF) based LEDGF/p75 dependent IN activity, IN-LEDGF/p75 binding, and LEDGF/p75 independent 3' processing assays were carried out as previously described [32]. The HTRF signal was recorded using a Perkin Elmer Multimode EnSpire plate reader. The fitted dose-response curves were

generated to calculate  $IC_{50}$  using Origin software (OriginLab, Inc.). All fitted curves displayed a  $R^2$  of 0.99 or greater.

#### 4.5 Antiviral Activity and Cytotoxicity Assays

The indicated concentrations of the test compounds or diluent control (DMSO) were added directly to the target cells and the cells were infected with untreated virions. HeLa TZM-bl cells ( $2 \times 10^5$  cells/well of a 6-well plate in 2 ml of complete medium) were pre-incubated with the indicated concentrations of the test inhibitor or diluent control (DMSO) for 2 h. The cells were then infected with HIV-1 virions equivalent to 4 ng of HIV-1 p24 as determined by HIV-1 Gag p24 ELISA (ZeptoMetrix) following manufacturer's protocol. Two hours post-infection the culture supernatant was removed, washed once with complete medium, and then fresh complete medium was added with the inhibitor concentration maintained. The cells were cultured for 48 h and the cell extracts were prepared using 16 reporter lysis buffer (Promega). Luciferase activity was determined using a commercially available kit (Promega). The cytotoxicity assays were performed as described previously [28]. The fitted dose-response curves were generated to calculate  $EC_{50}$  or  $CC_{50}$  using Origin software (OriginLab, Inc.). All fitted curves displayed a  $R^2$  of 0.97 or greater.

#### Acknowledgements

We are grateful to Dr. Ross C. Larue for critical reading of the manuscript and helpful comments. These studies were in part supported by University of Messina Research&Mobility 2015 Project (project code RES\_AND\_MOB\_2015\_DE\_LUCA) and by National Institutes of Health grant R01AI110310 (to M.K. and J.R.F.)

#### References

- [1] M. Jaskolski, J.N. Alexandratos, G. Bujacz, A. Wlodawer, Piecing together the structure of retroviral integrase, an important target in AIDS therapy, *FEBS J* 276 (2009) 2926-2946.
- [2] L. Feng, R.C. Larue, A. Slaughter, J.J. Kessl, M. Kvaratskhelia, HIV-1 integrase multimerization as a therapeutic target, *Curr Top Microbiol Immunol* 389 (2015) 93-119.
- [3] T. Wills, V. Vega, Elvitegravir: a once-daily inhibitor of HIV-1 integrase, *Expert Opin Investig Drugs* 21 (2012) 395-401.
- [4] FDA approves raltegravir tablets, *AIDS Patient Care STDS* 21 (2007) 889.
- [5] S.L. Karmon, M. Markowitz, Next-generation integrase inhibitors : where to after raltegravir?, *Drugs* 73 (2013) 213-228.
- [6] V. Summa, A. Petrocchi, F. Bonelli, B. Crescenzi, M. Donghi, M. Ferrara, F. Fiore, C. Gardelli, O. Gonzalez Paz, D.J. Hazuda, P. Jones, O. Kinzel, R. Laufer, E. Monteagudo, E. Muraglia, E. Nizi, F. Orvieto, P. Pace, G. Pescatore, R. Scarpelli, K. Stillmock, M.V. Witmer, M. Rowley, *Discovery*

of raltegravir, a potent, selective orally bioavailable HIV-integrase inhibitor for the treatment of HIV-AIDS infection, *J Med Chem* 51 (2008) 5843-5855.

[7] J. van Lunzen, F. Maggiolo, J.R. Arribas, A. Rakhmanova, P. Yeni, B. Young, J.K. Rockstroh, S. Almond, I. Song, C. Brothers, S. Min, Once daily dolutegravir (S/GSK1349572) in combination therapy in antiretroviral-naive adults with HIV: planned interim 48 week results from SPRING-1, a dose-ranging, randomised, phase 2b trial, *Lancet Infect Dis* 12 (2012) 111-118.

[8] K.K. Pandey, Critical appraisal of elvitegravir in the treatment of HIV-1/AIDS, *HIV AIDS (Auckl)* 6 (2014) 81-90.

[9] N. Sichtig, S. Sierra, R. Kaiser, M. Daumer, S. Reuter, E. Schuler, A. Altmann, G. Fatkenheuer, U. Dittmer, H. Pfister, S. Esser, Evolution of raltegravir resistance during therapy, *J Antimicrob Chemother* 64 (2009) 25-32.

[10] R.T. Steigbigel, D.A. Cooper, P.N. Kumar, J.E. Eron, M. Schechter, M. Markowitz, M.R. Loutfy, J.L. Lennox, J.M. Gatell, J.K. Rockstroh, C. Katlama, P. Yeni, A. Lazzarin, B. Clotet, J. Zhao, J. Chen, D.M. Ryan, R.R. Rhodes, J.A. Killar, L.R. Gilde, K.M. Strohmaier, A.R. Meibohm, M.D. Miller, D.J. Hazuda, M.L. Nessel, M.J. DiNubile, R.D. Isaacs, B.Y. Nguyen, H. Teppler, B.S. Teams, Raltegravir with optimized background therapy for resistant HIV-1 infection, *N Engl J Med* 359 (2008) 339-354.

[11] M. Metifiot, N. Vandegraaff, K. Maddali, A. Naumova, X. Zhang, D. Rhodes, C. Marchand, Y. Pommier, Elvitegravir overcomes resistance to raltegravir induced by integrase mutation Y143, *AIDS* 25 (2011) 1175-1178.

[12] M. Li, M. Mizuuchi, T.R. Burke, Jr., R. Craigie, Retroviral DNA integration: reaction pathway and critical intermediates, *EMBO J* 25 (2006) 1295-1304.

[13] L. Krishnan, A. Engelman, Retroviral integrase proteins and HIV-1 DNA integration, *J Biol Chem* 287 (2012) 40858-40866.

[14] A. Engelman, P. Cherepanov, The structural biology of HIV-1: mechanistic and therapeutic insights, *Nat Rev Microbiol* 10 (2012) 279-290.

[15] P. Cherepanov, G. Maertens, P. Proost, B. Devreese, J. Van Beeumen, Y. Engelborghs, E. De Clercq, Z. Debyser, HIV-1 integrase forms stable tetramers and associates with LEDGF/p75 protein in human cells, *J Biol Chem* 278 (2003) 372-381.

[16] A. Ciuffi, M. Llano, E. Poeschla, C. Hoffmann, J. Leipzig, P. Shinn, J.R. Ecker, F. Bushman, A role for LEDGF/p75 in targeting HIV DNA integration, *Nat Med* 11 (2005) 1287-1289.

[17] M. Llano, D.T. Saenz, A. Meehan, P. Wongthida, M. Peretz, W.H. Walker, W. Teo, E.M. Poeschla, An essential role for LEDGF/p75 in HIV integration, *Science* 314 (2006) 461-464.

[18] M.C. Shun, N.K. Raghavendra, N. Vandegraaff, J.E. Daigle, S. Hughes, P. Kellam, P. Cherepanov, A. Engelman, LEDGF/p75 functions downstream from preintegration complex formation to effect gene-specific HIV-1 integration, *Genes Dev* 21 (2007) 1767-1778.

[19] K. Busschots, J. Vercammen, S. Emiliani, R. Benarous, Y. Engelborghs, F. Christ, Z. Debyser, The interaction of LEDGF/p75 with integrase is lentivirus-specific and promotes DNA binding, *J Biol Chem* 280 (2005) 17841-17847.

[20] M. Llano, J. Morrison, E.M. Poeschla, Virological and cellular roles of the transcriptional coactivator LEDGF/p75, *Curr Top Microbiol Immunol* 339 (2009) 125-146.

[21] L.Q. Al-Mawsawi, N. Neamati, Blocking interactions between HIV-1 integrase and cellular cofactors: an emerging anti-retroviral strategy, *Trends Pharmacol Sci* 28 (2007) 526-535.

[22] A. Engelman, P. Cherepanov, The lentiviral integrase binding protein LEDGF/p75 and HIV-1 replication, *PLoS Pathog* 4 (2008) e1000046.

[23] P. Cherepanov, E. Devroe, P.A. Silver, A. Engelman, Identification of an evolutionarily conserved domain in human lens epithelium-derived growth factor/transcriptional co-activator p75 (LEDGF/p75) that binds HIV-1 integrase, *J Biol Chem* 279 (2004) 48883-48892.

- [24] P. Cherepanov, A.L. Ambrosio, S. Rahman, T. Ellenberger, A. Engelman, Structural basis for the recognition between HIV-1 integrase and transcriptional coactivator p75, *Proc. Natl. Acad. Sci. U S A* 102 (2005) 17308-17313.
- [25] F. Christ, A. Voet, A. Marchand, S. Nicolet, B.A. Desimmie, D. Marchand, D. Bardiot, N.J. Van der Veken, B. Van Remoortel, S.V. Strelkov, M. De Maeyer, P. Chaltin, Z. Debyser, Rational design of small-molecule inhibitors of the LEDGF/p75-integrase interaction and HIV replication, *Nat Chem Biol* 6 (2010) 442-448.
- [26] L.D. Fader, E. Malenfant, M. Parisien, R. Carson, F. Bilodeau, S. Landry, M. Pesant, C. Brochu, S. Morin, C. Chabot, T. Halmos, Y. Bousquet, M.D. Bailey, S.H. Kawai, R. Coulombe, S. LaPlante, A. Jakalian, P.K. Bhardwaj, D. Wernic, P. Schroeder, M. Amad, P. Edwards, M. Garneau, J. Duan, M. Cordingley, R. Bethell, S.W. Mason, M. Bos, P. Bonneau, M.A. Poupart, A.M. Faucher, B. Simoneau, C. Fenwick, C. Yoakim, Y. Tsantrizos, Discovery of BI 224436, a Nucleoside Site Integrase Inhibitor (NCINI) of HIV-1, *ACS Med Chem Lett* 5 (2014) 422-427.
- [27] M. Tsiang, G.S. Jones, A. Niedziela-Majka, E. Kan, E.B. Lansdon, W. Huang, M. Hung, D. Samuel, N. Novikov, Y. Xu, M. Mitchell, H. Guo, K. Babaoglu, X. Liu, R. Geleziunas, R. Sakowicz, New class of HIV-1 integrase (IN) inhibitors with a dual mode of action, *J Biol Chem* 287 (2012) 21189-21203.
- [28] A. Sharma, A. Slaughter, N. Jena, L. Feng, J.J. Kessl, H.J. Fadel, N. Malani, F. Male, L. Wu, E. Poeschla, F.D. Bushman, J.R. Fuchs, M. Kvaratskhelia, A New Class of Multimerization Selective Inhibitors of HIV-1 Integrase, *PLoS Pathog* 10 (2014) e1004171.
- [29] E. Le Rouzic, D. Bonnard, S. Chasset, J.M. Bruneau, F. Chevreuil, F. Le Strat, J. Nguyen, R. Beauvoir, C. Amadori, J. Brias, S. Vomscheid, S. Eiler, N. Levy, O. Delelis, E. Deprez, A. Saib, A. Zamborlini, S. Emiliani, M. Ruff, B. Ledoussal, F. Moreau, R. Benarous, Dual inhibition of HIV-1 replication by integrase-LEDGF allosteric inhibitors is predominant at the post-integration stage, *Retrovirology* 10 (2013) 144.
- [30] N. van Bel, Y. van der Velden, D. Bonnard, E. Le Rouzic, A.T. Das, R. Benarous, B. Berkhout, The allosteric HIV-1 integrase inhibitor BI-D affects virion maturation but does not influence packaging of a functional RNA genome, *PLoS One* 9 (2014) e103552.
- [31] P. Cherepanov, A.L. Ambrosio, S. Rahman, T. Ellenberger, A. Engelman, Structural basis for the recognition between HIV-1 integrase and transcriptional coactivator p75, *Proc Natl Acad Sci U S A* 102 (2005) 17308-17313.
- [32] J.J. Kessl, N. Jena, Y. Koh, H. Taskent-Sezgin, A. Slaughter, L. Feng, S. de Silva, L. Wu, S.F. Le Grice, A. Engelman, J.R. Fuchs, M. Kvaratskhelia, A multimode, cooperative mechanism of action of allosteric HIV-1 integrase inhibitors, *J Biol Chem* 287 (2012) 16801-16811.
- [33] K.A. Jurado, A. Engelman, Multimodal mechanism of action of allosteric HIV-1 integrase inhibitors, *Expert Rev Mol Med* 15 (2013) e14.
- [34] K.A. Jurado, H. Wang, A. Slaughter, L. Feng, J.J. Kessl, Y. Koh, W. Wang, A. Ballandras-Colas, P.A. Patel, J.R. Fuchs, M. Kvaratskhelia, A. Engelman, Allosteric integrase inhibitor potency is determined through the inhibition of HIV-1 particle maturation, *Proc Natl Acad Sci U S A* 110 (2013) 8690-8695.
- [35] M. Balakrishnan, S.R. Yant, L. Tsai, C. O'Sullivan, R.A. Bam, A. Tsai, A. Niedziela-Majka, K.M. Stray, R. Sakowicz, T. Cihlar, Non-Catalytic Site HIV-1 Integrase Inhibitors Disrupt Core Maturation and Induce a Reverse Transcription Block in Target Cells, *PLoS One* 8 (2013) e74163.
- [36] B.A. Desimmie, R. Schrijvers, J. Demeulemeester, D. Borrenberghs, C. Weydert, W. Thys, S. Vets, B. Van Remoortel, J. Hofkens, J. De Rijck, J. Hendrix, N. Bannert, R. Gijssbers, F. Christ, Z. Debyser, LEDGINs inhibit late stage HIV-1 replication by modulating integrase multimerization in the virions, *Retrovirology* 10 (2013) 57.

- [37] J. Fontana, K.A. Jurado, N. Cheng, N.L. Ly, J.R. Fuchs, R.J. Gorelick, A.N. Engelman, A.C. Steven, Distribution and Redistribution of HIV-1 Nucleocapsid Protein in Immature, Mature, and Integrase-Inhibited Virions: a Role for Integrase in Maturation, *J Virol* 89 (2015) 9765-9780.
- [38] L. Feng, V. Dharmarajan, E. Serrao, A. Hoyte, R.C. Larue, A. Slaughter, A. Sharma, M.R. Plumb, J.J. Kessl, J.R. Fuchs, F.D. Bushman, A.N. Engelman, P.R. Griffin, M. Kvaratskhelia, The Competitive Interplay between Allosteric HIV-1 Integrase Inhibitor BI/D and LEDGF/p75 during the Early Stage of HIV-1 Replication Adversely Affects Inhibitor Potency, *ACS Chem Biol* (2016).
- [39] L. Feng, A. Sharma, A. Slaughter, N. Jena, Y. Koh, N. Shkriabai, R.C. Larue, P.A. Patel, H. Mitsuya, J.J. Kessl, A. Engelman, J.R. Fuchs, M. Kvaratskhelia, The A128T resistance mutation reveals aberrant protein multimerization as the primary mechanism of action of allosteric HIV-1 integrase inhibitors, *J Biol Chem* 288 (2013) 15813-15820.
- [40] A. Slaughter, K.A. Jurado, N. Deng, L. Feng, J.J. Kessl, N. Shkriabai, R.C. Larue, H.J. Fadel, P.A. Patel, N. Jena, J.R. Fuchs, E. Poeschla, R.M. Levy, A. Engelman, M. Kvaratskhelia, The mechanism of H171T resistance reveals the importance of N inverted question mark -protonated His171 for the binding of allosteric inhibitor BI-D to HIV-1 integrase, *Retrovirology* 11 (2014) 100.
- [41] D.J. Newman, G.M. Cragg, Natural products as sources of new drugs over the 30 years from 1981 to 2010, *J Nat Prod* 75 (2012) 311-335.
- [42] Y.W. Chin, M.J. Balunas, H.B. Chai, A.D. Kinghorn, Drug discovery from natural sources, *AAPS J* 8 (2006) E239-253.
- [43] L. De Luca, F. Morreale, F. Christ, Z. Debyser, S. Ferro, R. Gitto, New scaffolds of natural origin as Integrase-LEDGF/p75 interaction inhibitors: virtual screening and activity assays, *Eur J Med Chem* 68 (2013) 405-411.
- [44] L. De Luca, S. Ferro, F. Morreale, F. Christ, Z. Debyser, A. Chimirri, R. Gitto, Fragment hopping approach directed at design of HIV IN-LEDGF/p75 interaction inhibitors, *J Enzyme Inhib Med Chem* 28 (2013) 1002-1009.
- [45] S. Ferro, L. De Luca, F.E. Agharbaoui, F. Christ, Z. Debyser, R. Gitto, Optimization of rhodanine scaffold for the development of protein-protein interaction inhibitors, *Bioorg Med Chem* 23 (2015) 3208-3214.
- [46] G. Jones, P. Willett, R.C. Glen, A.R. Leach, R. Taylor, Development and validation of a genetic algorithm for flexible docking, *J Mol Biol* 267 (1997) 727-748.
- [47] D.A. Case, T.A. Darden, T.E. Cheatham, III, C.L. Simmerling, J. Wang, R.E. Duke, R. Luo, R.C. Walker, W. Zhang, K.M. Merz, B. Roberts, B. Wang, S. Hayik, A. Roitberg, G. Seabra, I. Kolossváry, K.F. Wong, F. Paesani, J. Vanicek, J. Liu, X. Wu, S.R. Brozell, T. Steinbrecher, H. Gohlke, Q. Cai, X. Ye, J. Wang, M.-J. Hsieh, G. Cui, D.R. Roe, D.H. Mathews, M.G. Seetin, C. Sagui, V. Babin, T. Luchko, S. Gusarov, A. Kovalenko, P.A. Kollman, AMBER 11, in, University of California, San Francisco, 2010.
- [48] L. De Luca, F. Morreale, A. Chimirri, Insight into the fundamental interactions between LEDGF binding site inhibitors and integrase combining docking and molecular dynamics simulations, *J Chem Inf Model* 52 (2012) 3245-3254.
- [49] D.S. Accelrys.
- [50] P.A. Kollman, I. Massova, C. Reyes, B. Kuhn, S. Huo, L. Chong, M. Lee, T. Lee, Y. Duan, W. Wang, O. Donini, P. Cieplak, J. Srinivasan, D.A. Case, T.E. Cheatham, 3rd, Calculating structures and free energies of complex molecules: combining molecular mechanics and continuum models, *Acc Chem Res* 33 (2000) 889-897.
- [51] S. Maignan, J.P. Guilloteau, Q. Zhou-Liu, C. Clement-Mella, V. Mikol, Crystal structures of the catalytic domain of HIV-1 integrase free and complexed with its metal cofactor: high level of similarity of the active site with other viral integrases, *J Mol Biol* 282 (1998) 359-368.
- [52] v.S.L.N.Y. Maestro, NY, 2009.

- [53] D.A.D. Case, T. A.; Cheatham, T. E.; III; Simmerling, C. L.; Wang, J.; Duke, R. E.; Luo, R.; Walker, R. C.; Zhang, W.; Merz, K. M.; Roberts, B.; Wang, B.; Hayik, S.; Roitberg, A.; Seabra, G.; Kolossváry, I.; Wong, K. F.; Paesani, F.; Vanicek, J.; Liu, J.; Wu, X.; Brozell, S. R.; Steinbrecher, T.; Gohlke, H.; Cai, Q.; Ye, X.; Wang, J.; Hsieh, M.-J.; Cui, G.; Roe, D. R.; Mathews, D. H.; Seetin, M. G.; Sagui, C.; Babin, V.; Luchko, T.; Gusarov, S.; Kovalenko, A.; Kollman, P. A.; University of California: San Francisco, 2010.
- [54] Y. Duan, C. Wu, S. Chowdhury, M.C. Lee, G. Xiong, W. Zhang, R. Yang, P. Cieplak, R. Luo, T. Lee, J. Caldwell, J. Wang, P. Kollman, A point-charge force field for molecular mechanics simulations of proteins based on condensed-phase quantum mechanical calculations, *J Comput Chem* 24 (2003) 1999-2012.
- [55] J. Wang, R.M. Wolf, J.W. Caldwell, P.A. Kollman, D.A. Case, Development and testing of a general amber force field, *J Comput Chem* 25 (2004) 1157-1174.
- [56] DeLano, W.L., DeLano Scientific LLC, The PyMOL Molecular Graphics System, San Carlos, CA, USA, 2008.

**Table 1.** Binding free energy estimation

Compound	R	$\Delta G_{\text{bind}}$ (complex 1)	$\Delta G_{\text{bind}}$ (complex 2)	$\Delta G_{\text{bind}}$ (Snapshots)
		Kcal/mol 2B4J-Ligand	Kcal/mol 3LPU-Ligand	2B4J-Ligand Kcal/mol
<b>Lavendustin B</b>		-15,39	-14,77	-18,09
<b>1</b>	H	-21,54	-19,41	-22,41
<b>2</b>	2-Cl	-25,73	-25,73	-24,99
<b>3</b>	3-Cl	-24,74	-24,41	-21,68
<b>4</b>	4-Cl	-21,33	-19,02	-17,75
<b>5</b>	2-F	-20,45	-20,64	-22,47
<b>6</b>	3-F	-20,10	-20,51	-20,08
<b>7</b>	4-F	-15,87	-16,00	-15,54
<b>8</b>	2-CH <sub>3</sub>	-22,24	-23,35	-21,40
<b>9</b>	3-CH <sub>3</sub>	-16,29	-15,09	-14,00
<b>10</b>	4-CH <sub>3</sub>	-12,86	-11,38	-12,65

$\Delta G_{\text{bind}}$  is the calculated binding free energy

**Table 2.** Hydrogen bonds analysis from the results of MD simulation for IN in complex with the designed compounds

Compound	IN in complex with	Donor	Acceptor	Occupancy (%) <sup>a</sup>	Distance (Å) <sup>b</sup>
Lavendustine B	Lavendustin B	Thr174(A) OH	O3	11.80	3.092 (0.21)
		Glu170(A) NH	O1	78.20	2.930 (0.18)
		Glu170(A) NH	O2	36.60	3.051 (0.22)
		His171(A) NH	O2	63.30	3.230 (0.18)
1	H	Thr174(A) OH	O	21.90	3.077 (0.21)
		Thr174(A) OH	O1	10.40	3.093 (0.26)
		Glu170(A) NH	O2	90.40	2.923 (0.17)
		Glu170(A) NH	O1	64.30	3.108 (0.22)
		His171(A) NH	O1	76.70	3.102 (0.19)
		Gln95(A) NH	O	10.40	3.140 (0.18)
2	2Cl	Thr174(A) OH	O	76.60	3.029 (0.20)
		Thr174(A) OH	O1	34.90	2.896 (0.25)
		Glu170(A) NH	O2	98.80	2.966 (0.18)
		Glu170(A) NH	O1	78.80	3.070 (0.20)
		His171(A) NH	O1	84.30	3.086 (0.19)
		Gln95(A) NH	O	37.20	3.102 (0.19)
3	3Cl	Thr174(A) OH	O2	72.30	3.024 (0.20)
		Glu170(A) NH	O1	86.40	2.907 (0.16)
		Glu170(A) NH	O	61.20	3.083 (0.20)
		His171(A) NH	O	77.70	3.073 (0.18)
4	4Cl	Thr174(A) OH	O1	21.30	2.958 (0.26)
		Glu170(A) NH	O1	63.60	2.944 (0.17)
		His171(A) NH	O1	25.60	3.206 (0.18)
		His171(A) NH	O	24.50	3.168 (0.20)
5	2F	Thr174(A) OH	O2	24.30	3.043 (0.27)
		Glu170(A) NH	O1	95.60	2.960 (0.18)
		Glu170(A) NH	O2	76.70	3.060 (0.20)
		His171(A) NH	O1	82.10	3.093 (0.18)
6	3F	Thr174(A) OH	O1	78.40	2.999 (0.26)
		Thr174(A) OH	O	17.90	3.093 (0.18)
		Glu170(A) NH	O1	57.40	2.933 (0.16)
		His171(A) NH	O1	21.20	3.173 (0.18)
		His171(A) NH	O	10.40	3.267 (0.17)
7	4F	Thr174(A) OH	O	45.50	2.978 (0.27)
		Glu170(A) NH	O	32.40	2.970 (0.20)
		His171(A) NH	O1	23.70	3.076 (0.19)
8	2CH <sub>3</sub>	Thr174(A) OH	O2	54.80	2.950 (0.26)
		Thr174(A) OH	O	17.40	3.164 (0.19)
		Glu170(A) NH	O1	96.80	2.866 (0.14)
		Glu170(A) NH	O2	49.00	3.173 (0.21)
		His171(A) NH	O2	46.00	3.210 (0.18)
9	3CH <sub>3</sub>	Glu170(A) NH	O	21.60	2.970 (0.19)
		His171(A) NH	O1	10.30	3.243 (0.17)
10	4CH <sub>3</sub>	Thr174(A) OH	O	28.57	3.206 (0.19)
		Thr174(A) OH	O1	23.81	3.316 (0.19)

		Glu170(A) NH	O1	50.00	2.884 ( 0.16)
		His171(A) NH	O	28.57	3.065 ( 0.18)
		His171(A) NH	O1	26.19	3.273( 0.14)

<sup>a</sup>The listed donor and acceptor pairs correspond to the hydrogen bonds occupancies during the simulation.

<sup>b</sup>The average distance with standard error (SE =standard deviation/N<sup>1/2</sup>) in parentheses between hydrogen-acceptor atom and hydrogen-donor atom in the investigated time period.

ACCEPTED MANUSCRIPT

**Table 3:** Inhibition of IN-LEDGF/p75 binding, LEDGF/p75 dependent integration, and LEDGF/p75 independent 3'-processing activity of the synthesized compounds

Compound	R	LEDGF/p75 Dependent IN Activity (IC <sub>50</sub> μM)	IN-LEDGF/p75 Binding (IC <sub>50</sub> μM)	3'P (IC <sub>50</sub> μM)
<b>1</b>	<b>H</b>	7.93 ± 0.79	8.75 ± 2.36	69.97 ± 10.27
<b>2</b>	<b>2-Cl</b>	3.78 ± 0.35	3.28 ± 0.80	25.62 ± 1.88
<b>3</b>	<b>3-Cl</b>	13.48 ± 4.45	19.50 ± 2.55	>70
<b>5</b>	<b>2-F</b>	9.00 ± 0.24	17.84 ± 4.25	63.05 ± 5.16
<b>6</b>	<b>3-F</b>	18.50 ± 2.19	20.83 ± 2.46	68.56
<b>8</b>	<b>2-CH<sub>3</sub></b>	14.66 ± 0.69	27.59 ± 3.98	>70
<b><sup>a</sup>Lavendustin B</b>		-	94.07	-

Data for IC<sub>50</sub> are given as the mean ± SD from at least three independent experiments.

<sup>a</sup>The IC<sub>50</sub> of Lavendustin B is reported elsewhere and was evaluated by alpha screen assays [43].

**Figure Captions**

**Figure 1:** **A)** Chemical structures of 5-[bis(2-hydroxybenzyl)amino]-2-hydroxybenzoic acid (Lavendustin B) **B)** Superimposition of Lavendustin B (green) and compound KF115 (cyan) in complex with IN CCD (PDB code 2B4J). Key residues of the pocket are presented. The figure was created using PyMOL [56]. **C)** Chemical structures of KF115. **D)** Substitutions on the parent molecule.

**Figure 2:** Superimposition of IN CCD with **A)** Lavendustin B (violet) and compound **1** (cyan); **B)** compounds **2** (green), **3** (cyan) and **4** (magenta); **C)** compounds **5** (green), **6** (cyan) and **7** (magenta); **D)** compounds **8** (green), **9** (cyan) and **10** (magenta). Key residues of the pocket are presented. The figure was created using PyMOL [56].

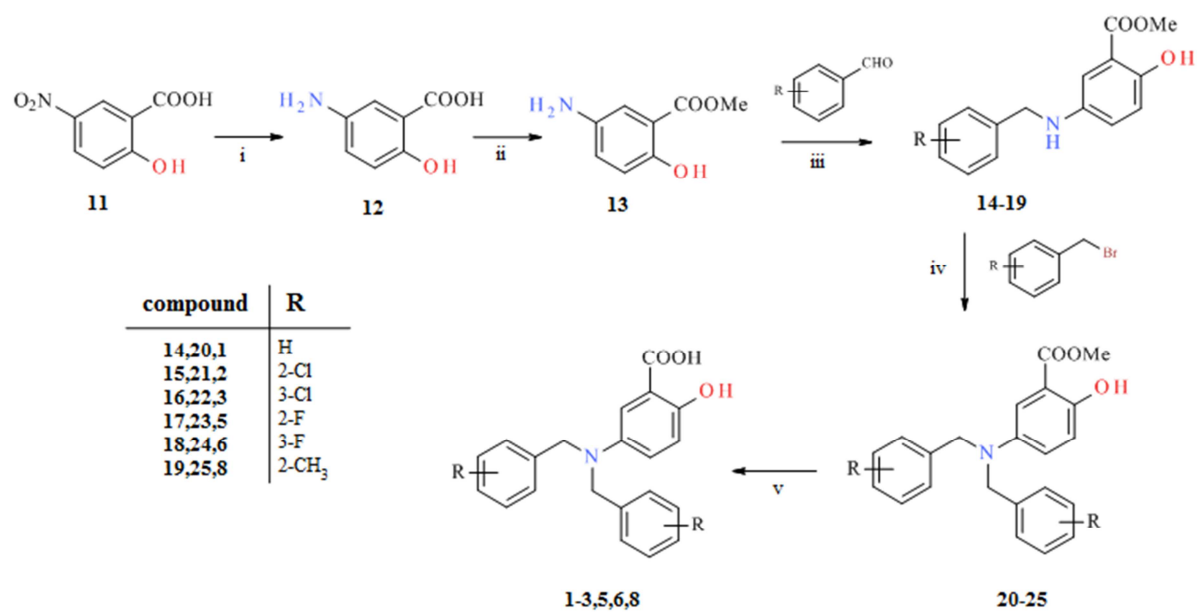
**Figure 3:** **A)** chemical structure of compound **2**; **B)** Curve fitting of inhibition of LEDGF/p75 dependent IN activity by compound **2** (black squares); **C)** Curve fitting of dose-dependent inhibition of IN-LEDGF binding by compound **2** (black squares); **D)** Curve fitting of dose-dependent inhibition of 3' processing by compound **2** (black squares). The average values from three independent experiments are shown for each assay.

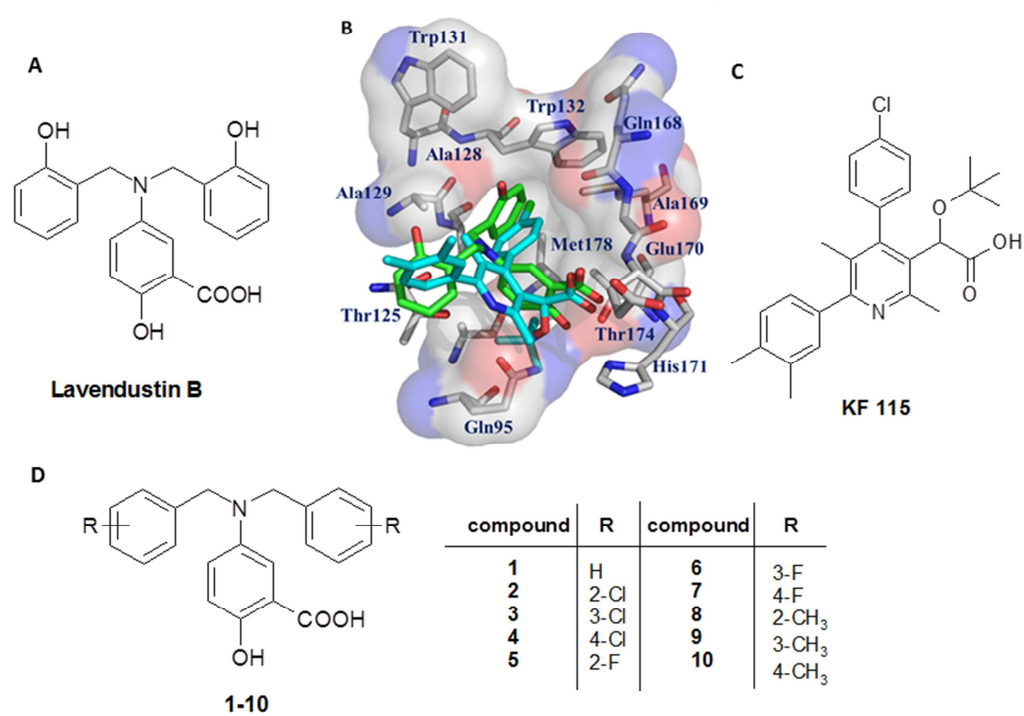
**Figure 4:** **A)** Luciferase quantification to measure the inhibition by compound **2** over the indicated concentrations. VSV-g pseudotyped virus was used to infect HEK293T cells under drug treatment. **B)** Cytotoxicity effect of compound **2** over the indicated concentrations without viral infection.

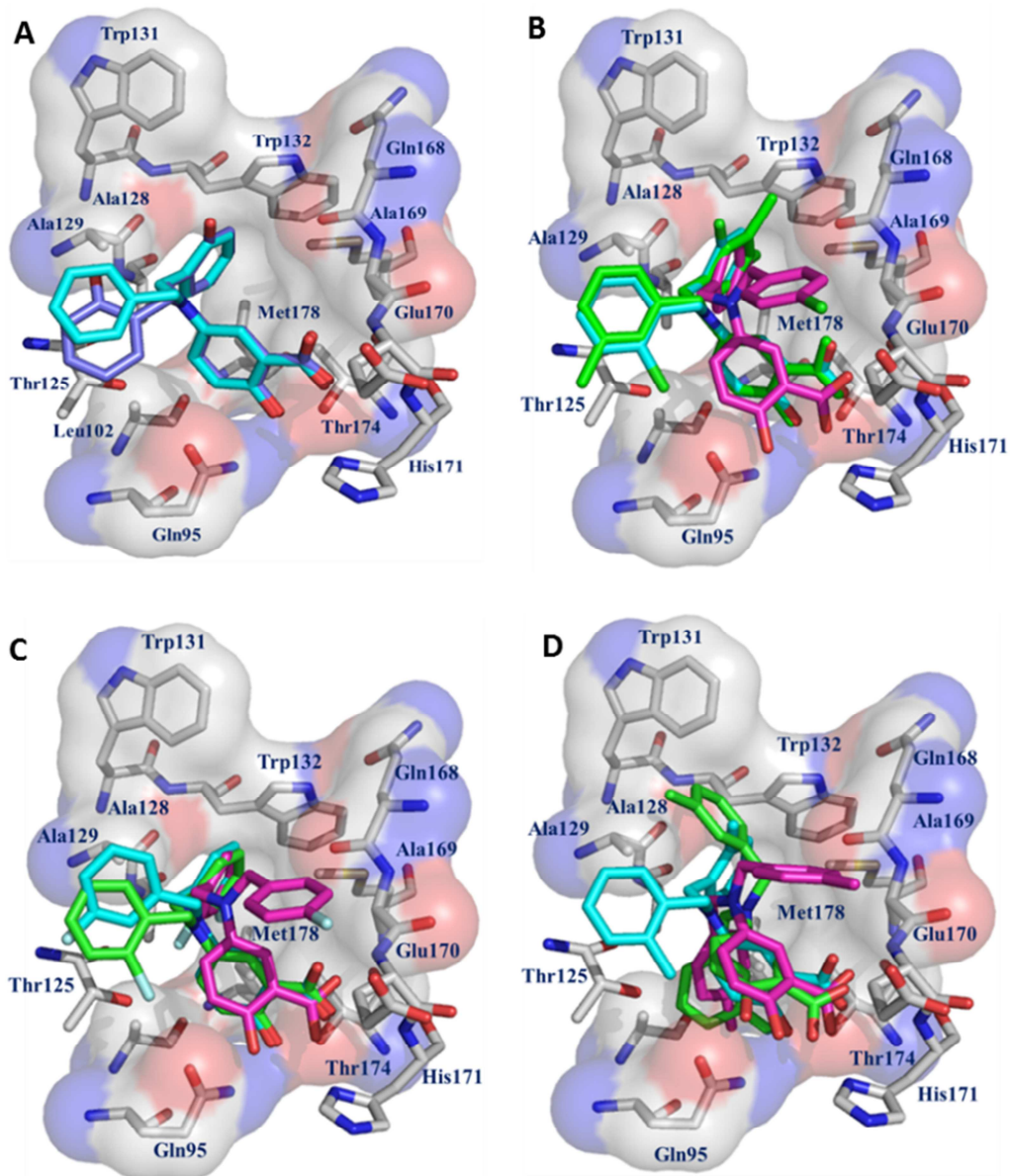
**Scheme 1**

**Reagents and conditions:** (i) Zinc dust, 0-5°C, HCl<sub>conc.</sub>, reflux, 4h; (ii) MeOH, H<sub>2</sub>SO<sub>4</sub>, 0°C, 80°C, 24h; (iii) MeOH, AcOH, 30', 40°C, rt 1h, 5-10 °C NaCNBH<sub>3</sub>, 2 h rt; (iv) NaH, DMF, Argon 3h rt; (v) NaOH, MeOH, THF, 60°C, 24h, HCl 2N.

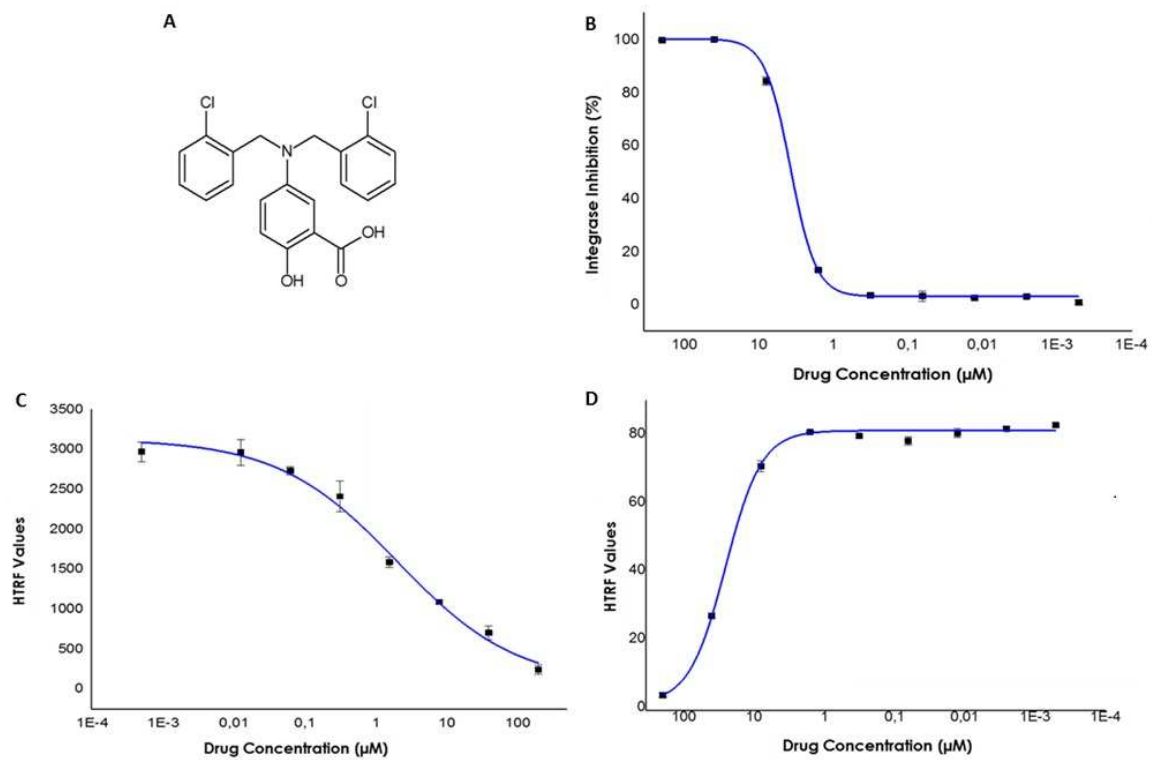
ACCEPTED MANUSCRIPT

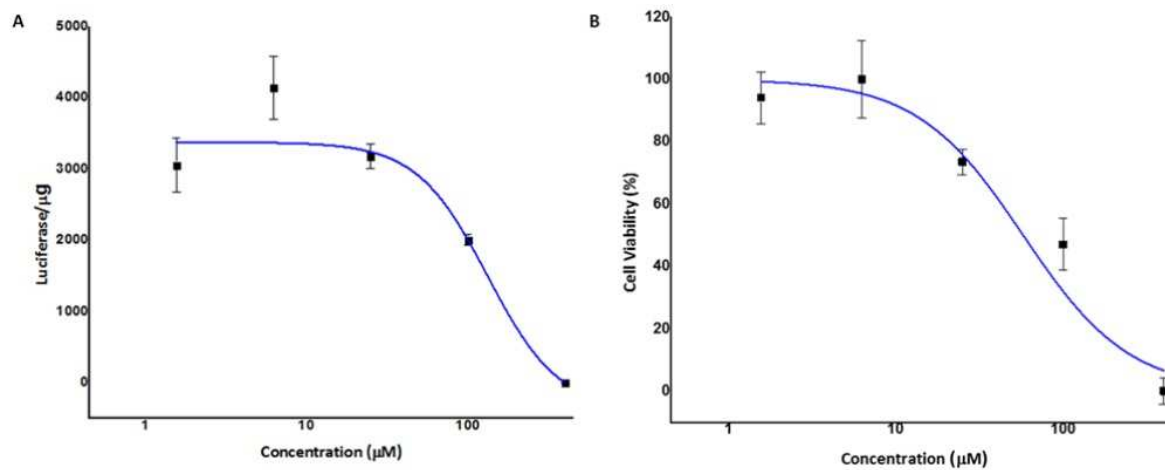






ACCE





## RESEARCH HIGHLIGHTS

**Computational and synthetic approaches for developing Lavendustin B derivatives as allosteric inhibitors of HIV-1 integrase**

Fatima E. Agharbaoui<sup>a,b,c</sup>, Ashley C. Hoyte<sup>b</sup>, Stefania Ferro<sup>a</sup>, Rosaria Gitto<sup>a</sup>, Maria Rosa Buemi<sup>a</sup>, James R. Fuchs<sup>c</sup>, Mamuka Kvaratskhelia<sup>b</sup>, Laura De Luca<sup>a,\*</sup>

- A computational workflow applying docking, rescoring, ultrashort MD simulations and hydrogen bond analysis was set up to evaluate the designed Lavendustin B derivatives as IN-LEDGF interaction inhibitors.
- The selected compounds were synthesized.
- The synthesized derivatives were evaluated using HTRF-assays and a promising lead was identified.